



# Lipid composition regulates the conformation and insertion of the antimicrobial peptide maculatin 1.1<sup>☆</sup>

Marc-Antoine Sani<sup>\*</sup>, Thomas C. Whitwell, Frances Separovic

School of Chemistry, Bio21 Institute, University of Melbourne, VIC 3010, Australia

## ARTICLE INFO

### Article history:

Received 14 May 2011

Received in revised form 12 July 2011

Accepted 14 July 2011

Available online 23 July 2011

### Keywords:

Circular dichroism

Oriented circular dichroism

Phospholipids

Antimicrobial peptide

Hydrophobic mismatch

Curvature

## ABSTRACT

Antimicrobial peptides interact with cell membranes and their selectivity is contingent on the nature of the constituent lipids. Eukaryotic and bacterial membranes are comprised of different proportions of a range of lipid species with different physical properties. Hence, characterisation of antimicrobial peptides with respect to the magnitude of their interactions with model membranes of different lipid types is needed. Maculatin 1.1 is a short antimicrobial peptide secreted from the skin of several Australian tree-frog species. Circular dichroism spectroscopy (CD) was used to explore the interaction of maculatin 1.1 with a wide range of model membrane systems of different head group and acyl chain characteristics. For neutral phosphatidylcholine (PC), unlike anionic phospholipids, the magnitude of the peptide interactions was dependent on the length and degree of saturation of the constituent acyl chains. Oriented circular dichroism (OCD) data indicated that helical structure was likely promoted by peptide insertion into the hydrophobic core of PC bilayers. The addition of cholesterol (30% mol/mol) tended to decrease the membrane interaction of maculatin 1.1. Anionic lipids locked maculatin 1.1 via electrostatic interactions onto the surface of oriented bilayers as seen in OCD spectra. Furthermore, increasing the membrane curvature by reducing the vesicle radii only slightly reduced the proportion of helical structure in all systems by approximately 10%. The peptide–lipid interaction was strongly dependent on both the lipid chain length and head group, which highlights the importance of the lipid composition used to mimic different cell types. This article is part of a Special Issue entitled: Membrane protein structure and function.

© 2011 Elsevier B.V. All rights reserved.

## 1. Introduction

Until recently, membrane lipids were often perceived as simple building blocks that compose cell membranes, and were not considered to play an important role in biological processes. Efforts in understanding the lipid diversity encountered in natural membranes have shown that the bewildering chemical composition of lipid membranes is certainly a key factor in the regulation of cellular mechanisms [1,2]. An example is the selective affinity of antimicrobial peptides (AMP) for specific bacterial membrane lipids [3]. However, the intrinsic complexity of natural membranes renders difficult to investigate *in vivo* the role

of individual lipids at molecular resolution. Therefore, *in vitro* studies using model membranes are commonly used. While this methodology has revealed the nature of lipid–AMP interaction [4], correlations of *in vitro* measurements with *in vivo* observations are often unsatisfactory, mainly due to the membrane composition used [5,6].

Bacterial membranes are composed primarily of three phospholipids: phosphatidylethanolamine (PE), phosphatidylglycerol (PG) and cardiolipin (CL), in species-specific proportions; and, depending on growth conditions, can have branched, cyclic, saturated or unsaturated aliphatic chains [3,7]. The biophysical properties of these membranes are, therefore, extremely complex, varied and poorly understood. The phospholipids of eukaryotic membranes are mainly phosphatidylcholine (PC), phosphatidylserine (PS), PE and CL (only present in mitochondria) with a high degree of unsaturation and can contain up to 30% (by mole) cholesterol [8,9]. Hence, it is crucial to define and use relevant lipid systems in order to understand the affinity and activity of AMP toward bacterial membranes.

In this study, we have focused on the conformation of the AMP maculatin 1.1 in a variety of lipid systems and highlight the importance of lipid selection when modelling biological membranes. Using circular dichroism (CD) spectroscopy as a rapid scanning technique, we found that, in addition to electrostatic interactions, the hydrophobic core of membranes may be critical for the formation of

**Abbreviations:** AMP, Antimicrobial peptide; CD, Circular dichroism; Chol, Cholesterol; CL, Cardiolipin; DD, Didecanoyl (C10:0); DH, Dihexanoyl (C6:0); DL, Dilauroyl (12:0); DM, Dimyristoyl (C14:0); DO, Dioleoyl (C18:1); DP, Dipalmitoyl (C16:0); DS, Distearoyl (C18:0); LPG, Lysophosphatidylglycerol; LUV, Large unilamellar vesicle; OCD, Oriented circular dichroism; PA, Phosphatidic acid; PC, Phosphatidylcholine; PE, Phosphatidylethanolamine; PG, Phosphatidylglycerol; PO, Palmitoyloleoyl (C16:0, 18:1); PS, Phosphatidylserine; SDS, Sodium dodecylsulfate; SUV, Small unilamellar vesicle; TFE, Trifluoroethanol; TM, Tetramyristoyl (C14:0).

<sup>☆</sup> This article is part of a Special Issue entitled: Membrane protein structure and function.

<sup>\*</sup> Corresponding author. Tel.: +61 3 8344 2436; fax: +61 3 9347 5180.

E-mail address: [msani@unimelb.edu.au](mailto:msani@unimelb.edu.au) (M.-A. Sani).

the active AMP structure. A relationship was identified between acyl chain length and the magnitude of the interaction of maculatin 1.1 with phospholipid membranes. The addition of cholesterol to the membrane systems appeared to have minimal effect on the peptide affinity or membrane interaction. Oriented circular dichroism (OCD) spectra were also obtained to monitor the ability of the peptide to insert into the hydrophobic core of planar membranes. Furthermore, the effect of curvature on the ability of maculatin 1.1 to adopt a helical structure was investigated by comparing large unilamellar vesicle (LUV) and small unilamellar vesicle (SUV) lipid systems.

## 2. Materials and methods

### 2.1. Materials

Maculatin 1.1 (GLFGVLAKVAHVPAIAEHF-NH<sub>2</sub>; MW 2148) with a >95% purity was purchased from Mimotopes Ltd. (Melbourne, Australia) and from the Bio21 Institute peptide facility (Melbourne, Australia). The peptide was washed in 5 mM HCl solution and lyophilised over-night to remove residual trifluoroacetic acid as described by Sani et al. [10]. All phospholipids were purchased from Avanti Polar Lipids (Alabaster, USA), except DDPG, DLPC, egg PC and cholesterol, which were obtained from Sigma (St Louis, USA), and used without further purification.

### 2.2. Sample preparation

Maculatin 1.1 was dissolved in Milli-Q water to afford a 1 mg/mL stock solution. The stock solution was sonicated and vortexed before each use. To prepare vesicles comprising a single lipid-type, lipids were re-suspended in 10 mM Tris and 20 mM NaCl buffer solution (pH 7.3) to produce 5 mM dispersions and subjected to three freeze/thaw cycles. The homogeneous dispersions were then extruded 10 times through an Avanti Mini-Extruder (Alabaster, USA) using 0.1 µm polycarbonate filters to produce LUVs of 100 nm diameter. Samples were extruded above the corresponding gel to fluid phase transition temperatures. For the preparation of LUV including 30% (by mole) of cholesterol, lipids and cholesterol were co-dissolved in chloroform/methanol (3:1 (v/v)) before removal of solvents by rotary evaporation. Lipid films were then hydrated with Milli-Q water and lyophilised over-night. The resultant lipid powders were re-suspended and extruded as described above. For the preparation of SUV (with the exception of DSPC where multilamellar vesicles were used due to difficulty with dispersion), LUV suspensions were pulse sonicated using a Branson sonifier (Danbury, USA) on ice for 10 min with a 40% duty

cycle to produce clear suspensions followed by centrifugation at 12,000 rpm to remove any titanium particles.

### 2.3. CD measurements

#### 2.3.1. Circular dichroism

Appropriate volumes of peptide and lipid vesicles were mixed to produce 300 µL samples with lipid to peptide molar ratio 30:1. Samples were allowed to equilibrate at the desired temperature prior to CD measurement. Spectra of the peptide stock solution were acquired before each lipid study and no significant changes were observed. Spectra were acquired on a Jasco J-815 spectropolarimeter (Jasco, Easton, MD, USA) between 198 and 250 nm using a 1 mm path-length quartz cell (Hainault, UK). Data below 198 nm was neglected because of high levels of scattering by the buffer solution containing NaCl salt. The experiments were run at 50 nm/min with 1 nm data intervals, an 8 s integration time and a 1 nm slit-width. Three accumulations were made to reduce noise. Signal was recorded as milli-degrees.

#### 2.3.2. Oriented circular dichroism

Oriented samples were prepared on a 0.5 mm quartz cell from Starna (Hainault, UK) previously washed with nitric acid and thoroughly rinsed with deionized water. Samples were prepared as previously described for the CD measurements before being deposited onto the quartz glass cell and dried overnight in an oven at 30% relative humidity. Samples were subsequently placed in a hydration chamber with saturated KCl solution for approximately 2 days. Lipid-only samples were prepared using the same procedure. Oriented circular dichroism (OCD) spectra were acquired on a Jasco J-815 spectropolarimeter (Jasco, Easton, USA). Spectra were recorded from 190 to 250 nm using a 2 nm bandwidth and three accumulations. Four different angles were used to correct any spectral artefacts due to linear dichroism and birefringence that could be caused by imperfections in the sample or strain in the quartz glass plate.

#### 2.3.3. CD spectral deconvolution

Spectra were zeroed at 250 nm and normalised to give units of mean-residue ellipticity (MRE) according to  $[\theta]_{\text{MRE}} = \theta / (c \times l \times N_r)$ , where  $\theta$  is the recorded ellipticity in millidegrees,  $c$  is the peptide concentration in  $\text{dmol.L}^{-1}$ ,  $l$  is the cell path-length in cm and  $N_r$  is the number of residue per peptide. The secondary structure was calculated from processed CD spectra using the CDPro Software Package with the ContinLL algorithm and the SMP56 basis-set [11–13].

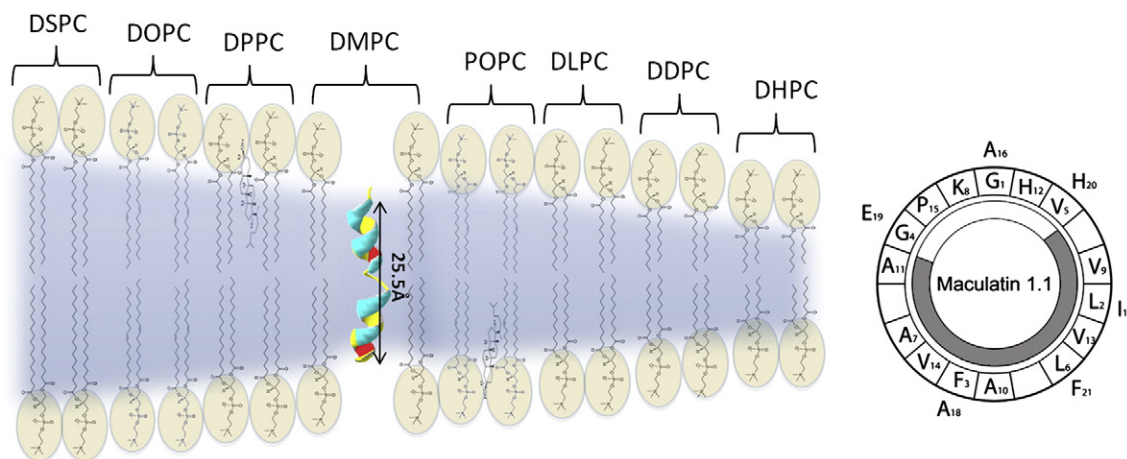


**Fig. 1.** Schematic of the hydrophobic core of several PC lipids scaled to the length of maculatin 1.1 obtained from the NMR structure in TFE/H<sub>2</sub>O solution [14]. The Edmundson wheel is displayed to show the amphipathic character of maculatin 1.1.

### 3. Results

#### 3.1. Maculatin 1.1 conformation in buffer and micelles

Balla et al. have previously shown that maculatin 1.1 is unstructured in solution and adopts an  $\alpha$ -helical conformation in trifluoroethanol (TFE) or upon interaction with DPC micelles [14]. The helical wheel representing the conformation of maculatin 1.1 (Fig. 1) displays the amphipathic character known to promote the antimicrobial properties against bacteria [3–7]. The  $\alpha$ -helix proportion could, therefore, be used as a measure of the peptide affinity for specific lipid environments. As expected, the CD spectrum of maculatin 1.1 in buffer alone was dominated by a minimum at ~200 nm, characteristic of the random coil conformation; while in TFE, two minima at 222 nm and 209 nm and a maximum (truncated) at 200 nm, were observed as is usual for  $\alpha$ -helical structures (Fig. 2). No significant difference was observed between measurements done at 20 °C and 37 °C. The secondary structure analysis obtained by deconvolution gave 7% and 59%  $\alpha$ -helix in water and TFE, respectively (Table 1). Note that deconvolution values are not absolute values of monomeric population with a pure secondary structure but an average of intra- and inter-molecular conformations. Furthermore, values are considered to have an estimated error of  $\pm 5\%$ .

Strong interactions were observed with anionic SDS and LPG micelles at a lipid to peptide molar ratio of 30:1, almost promoting an identical amount of helical structure, at ~60%, whereas neutral DPC micelles reduced the  $\alpha$ -helix content to 32%.

#### 3.2. Maculatin 1.1 interaction with phosphatidylcholine vesicles

Phosphatidylcholine lipids bear an overall neutral charge (zwitterionic headgroup) and are often used to assess the hydrophobic interaction between peptides and membranes, as the electrostatic interactions with the surface are considerably reduced. Acyl chain length and degree of unsaturation were varied in order to investigate the ability of maculatin 1.1 to penetrate into the core of membranes depending on their hydrophobic thickness and fluidity. Except for DSPC, where SUV were used, all data presented in Table 1 were obtained with LUV of 100 nm diameter. Also, gel and fluid phases were investigated by acquiring the CD spectra below and above the main phase transition temperatures, when applicable.

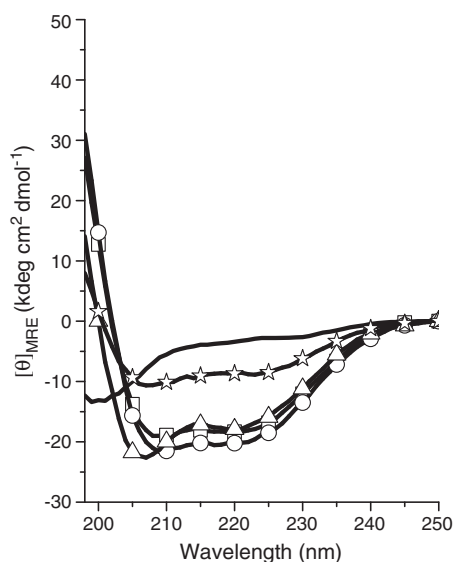


**Fig. 2.** CD spectra of maculatin 1.1 in: buffer only (no symbols); TFE solvent (triangles); SDS micelles (squares); LPG micelles (circles); and DPC micelles (stars). Spectra are an average of 3 accumulations recorded at 37 °C.

**Table 1**

Maculatin 1.1<sup>a</sup> secondary structure analyses<sup>b</sup> in LUV environment.

System (T <sub>m</sub> °C) [18,19]	T (°C) below T <sub>m</sub>	% $\alpha$ Helix	T (°C) above T <sub>m</sub>	% $\alpha$ Helix	Insertion <sup>c</sup>
Buffer	20	7	37	4	–
TFE	20	50	37	59	–
<i>Micelle systems</i>					
SDS (C12:0)	20	60	37	63	–
LPG (C16:0)	20	63	37	61	–
DPC (C12:0)	20	32	37	32	–
<i>Saturated neutral systems</i>					
LUV DHPC	–	–	37	7	no
LUV DDPC	–	–	37	59	yes
LUV DLPC (–1)	–	–	37	68	–
LUV DMPC (23)	10	78	37	73	yes
LUV DPPC (41)	20	14	60	64	–
Oriented DSPC <sup>†</sup> (55)	–	–	–	–	no
<i>Unsaturated neutral systems</i>					
LUV POPC (–2)	–	–	37	66	yes
LUV DOPC (–20)	–	–	37	60	–
LUV egg PC (–5)	–	–	37	52	–
<i>Cholesterol containing systems<sup>d</sup></i>					
LUV DMPC/Chol	10	29	37	61	yes
LUV DPPC/Chol	20	6	60	58	–
LUV POPC/Chol	–	–	37	70	yes
<i>Saturated anionic systems</i>					
LUV DMPA (50)	37	60	60	64	–
LUV DMPS (35)	20	70	45	73	–
LUV DPPS (54)	37	67	60	70	–
LUV DMPG (23)	10	77	37	63	very weak
LUV TMCL (42)	20	72	60	66	–
<i>Unsaturated anionic systems</i>					
LUV POPS (14)	10	79	37	65	–
LUV POPG (–2)	–	–	37	75	no
LUV <i>E. coli</i> PG	–	–	37	69	no
LUV <i>E. coli</i> CL	–	–	37	67	–

<sup>a</sup> The peptide concentration was 30  $\mu$ M. Buffer composition: 30  $\mu$ M in Tris 10 mM/NaCl 20 mM buffer pH=7.3. The lipid to peptide molar ratio was 30:1 for all systems.

<sup>b</sup> Deconvoluted with ContinLL algorithm and SDP 48 basis-set (CDPro software).

<sup>c</sup> Determined by OCD where 4 angles were averaged (see Section 2.3.2 and Fig. 4).

<sup>d</sup> 30% molar ratio of cholesterol to lipid. CD spectra were acquired above and below the T<sub>m</sub> of the lipid in the absence of cholesterol.

<sup>†</sup> DSPC would not disperse homogeneously in buffer and could not be extruded to form LUV so oriented bilayers were formed from SUV.

Except with extruded LUV of DHPC, where maculatin 1.1 exhibited a similar lineshape to that encountered in buffer, typical  $\alpha$ -helical spectra were obtained with all PC systems with intensity variations as seen in Fig. 3. The short chain DHPC (C6:0) showed little interaction with maculatin 1.1 at 37 °C (7% helix) but an increase was observed from DDPC (C10:0) to DMPC (C14:0), reaching 73% helical conformation. DPPC (C16:0) LUV produced a slight decrease in  $\alpha$ -helix to 64% (Table 1).

Interestingly, in the gel phase, where the lipid acyl chains are in an extended configuration, the amount of helical structure increased slightly in DMPC (at 10 °C) to 78% while dropping dramatically to 14% in DPPC (at 20 °C).

In order to control the fluidity of membranes, which is critical in many biological processes such as cell division or biomolecular diffusion, living organisms balance the amount of saturated and unsaturated lipids according to external conditions such as temperature–homeoviscous adaptation [15,16]. The interaction between maculatin 1.1 and unsaturated PC lipids was investigated with POPC (C16:0, 18:1), DOPC (di C18:1) and egg PC (which is a mixture of PC lipids extracted from chicken egg yolk with a predominance of POPC). Maculatin 1.1 adopted a largely helical conformation in unsaturated

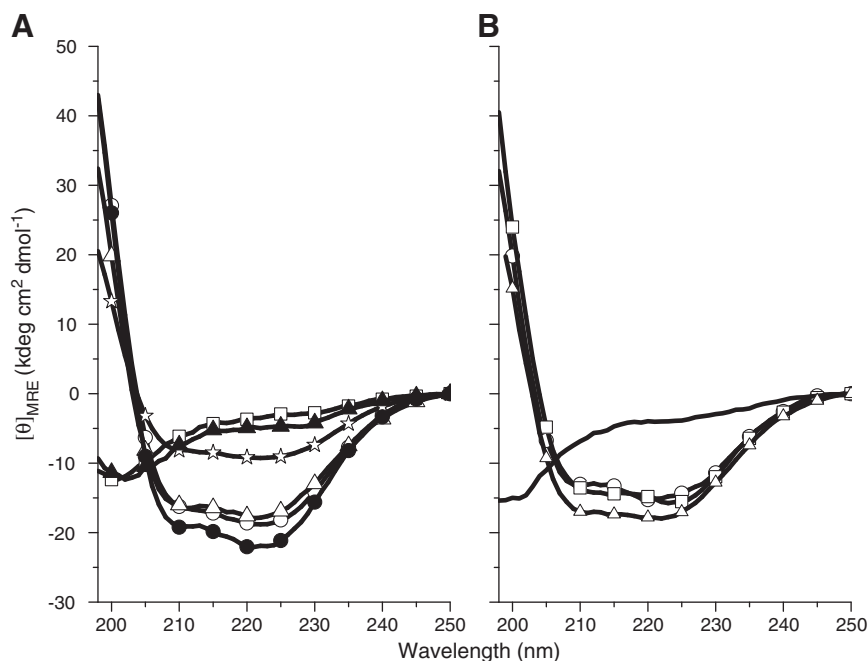


**Fig. 3.** CD spectra of maculatin 1.1 in LUV composed of: (A) DHPC (open squares); DMPC T=37 °C (open circles); DMPC T=10 °C (filled circles); DPPC T=60 °C (open triangles); DPPC T=20 °C (filled triangles); DSPC (stars); and (B) buffer only (no symbols); DOPC (squares); POPC (circles); egg PC (triangles). Spectra are an average of 3 accumulations.

phospholipid systems as displayed in the well-defined  $\alpha$ -helical CD lineshapes (Fig. 3, panel B). The heterogeneous acyl chain mixture of egg PC reduced by ~10% the  $\alpha$ -helical content compared to POPC or DOPC (Table 1).

### 3.3. Effect of cholesterol

Phosphatidylcholines are the major lipids in eukaryotic cells, thus many *in vitro* studies are conducted with PC only. The presence of cholesterol, absent in prokaryotic cells, is known to stabilise membranes and is involved in ordered domains or 'rafts', where proteins are regulated [17,18]. The effect of a 30% molar ratio of cholesterol to phospholipid was investigated in DMPC, DPPC and POPC bilayers at different temperatures. Although cholesterol is known to abrogate the phase transition temperature, systems containing cholesterol were measured above and below the  $T_m$  of the lipid in the absence of cholesterol where applicable (Fig. 4).

POPC/Chol at 37 °C and DPPC/Chol at 20 °C and 60 °C promoted no significant difference compared to cholesterol-free samples and gave similar helical proportions for the peptide. In contrast, the addition of cholesterol to DMPC bilayers led to a reduced interaction with maculatin 1.1. Indeed, the peptide  $\alpha$ -helical content was decreased by ~15% at 37 °C and dropped considerably at 10 °C to 29%.

### 3.4. Maculatin 1.1 interaction with anionic lipids

The effect of a negatively charged membrane surface was investigated using different anionic phospholipids to probe if the type of headgroup was also a critical parameter influencing the maculatin 1.1 secondary structure. Differences between these lipids are: phosphatidic acid (PA) has a charged phosphate group, phosphatidylglycerol (PG) has two hydroxyl groups, phosphatidylserine (PS) has an amine and one carboxylic group, and finally cardiolipin (CL) has two phosphate groups and a hydroxyl group. Therefore, not only the charge but also the bulk steric effect, the hydrogen bonding capacity and the effect of acyl chain length and unsaturation can be investigated.

The CD spectra obtained for maculatin 1.1 interacting with anionic phospholipids were all typical of an  $\alpha$ -helical lineshape, with some intensity variations between lipid species and temperatures (Fig. 5). The saturated lipids, DMPS and DPPS, induced a similar amount of  $\alpha$ -helix in the gel and fluid phases, around 70% (Table 1), while DMPG and TMCL bilayers promoted a slightly higher helical proportion in the gel phase at ~75% than in the fluid phase at ~65%.

CD spectra of maculatin 1.1 interacting with unsaturated anionic lipids displayed the most intense helical lineshapes (Fig. 5). LUV of POPG and POPS at 37 °C promoted 75% and 65%, respectively. Similar conformations (~67%  $\alpha$ -helix) were obtained in *E. coli* PG and *E. coli* CL systems, which have heterogeneous acyl chains. POPS has a gel to

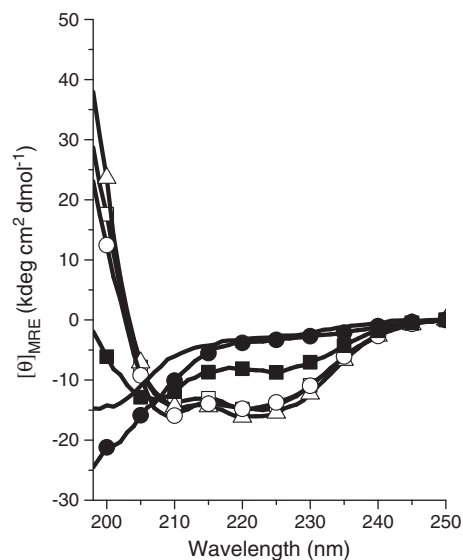


**Fig. 4.** CD spectra of maculatin 1.1 in buffer only (no symbol) and LUV composed of: DMPC/Chol T=37 °C (open squares); DMPC/Chol T=10 °C (filled squares); DPPC T=60 °C (open circles); DPPC T=20 °C (filled circles); and POPC/Chol (open triangle). Spectra are an average of 3 accumulations.



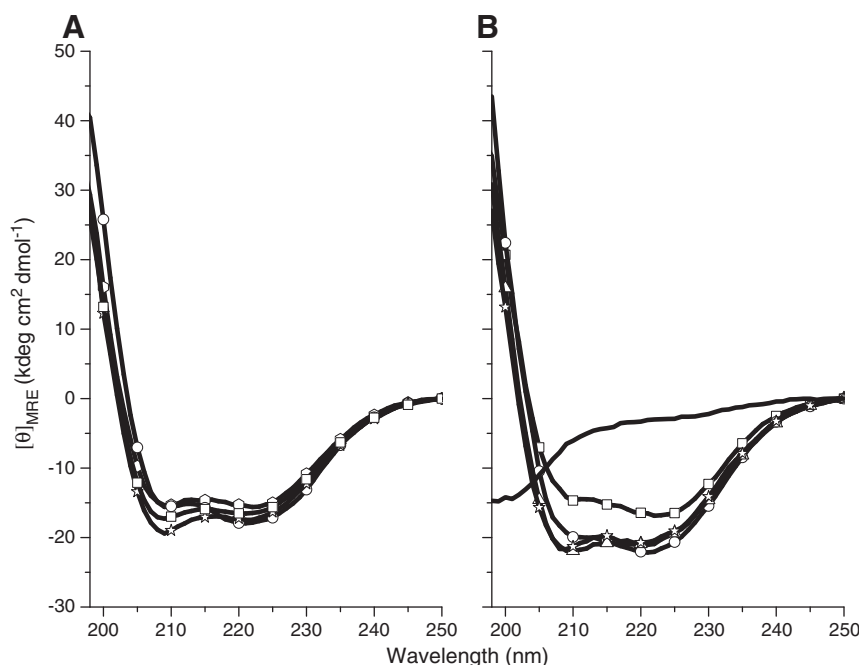


**Fig. 5.** CD spectra of maculatin 1.1 in LUV composed of: (A) DMPA (squares); DMPS (circles); DPPS (triangles); DMPG (hexagons); TMCL (stars); and (B) POPS (squares); POPG (circles); *E. coli* PG (triangles); *E. coli* CL (stars); buffer only (no symbol). Spectra are an average of 3 accumulations.

fluid phase transition temperature of 14 °C [19,20] and the highest proportion of  $\alpha$ -helix for maculatin 1.1 was obtained at 10 °C.

### 3.5. Effect of membrane curvature on maculatin 1.1 conformation

Membrane curvature is a factor known to influence peptide and protein structures [21]. To examine the effect of curvature on maculatin 1.1 conformation, CD experiments were performed with SUV systems. SUV have an average diameter of 15–30 nm, which increases the angle between the membrane surface and the helical structure; in other words the peptide must bend if contact with the surface is indispensable. The CD spectra of all SUV systems (not shown) were very similar to those observed with LUV. The secondary structure analyses obtained by deconvolution gave about 10% less helical structure (Table 2) for maculatin in SUV compared to LUV. Interestingly, Maculatin 1.1 did not interact strongly with DSPC SUV, promoting 37% of helical structure in the fluid phase (60°C) and only 23% in the gel phase (37°C).

### 3.6. Maculatin 1.1 insertion in oriented lipid membranes

Parallel and perpendicular peptide orientations relative to the membrane normal can be distinguished using oriented CD [22–24]. When transmembrane helical peptides are interacting with lipids forming planar bilayers on a glass plate, the OCD lineshape displays only the 222 nm minimum and the 190 nm maximum, the 208 nm band being suppressed in the interaction between the polarised beam and the oriented peptides. As described in Methods 2.3.2, to correct for birefringence and linear dichroism artefacts, the sample was rotated in the beam. The same buffer, lipid to peptide ratio and peptide concentration as for the fully hydrated samples were used. Experiments were performed at 37 °C.

Maculatin 1.1 did not orient in a short chain DHPC lipid (not shown) nor in a long chain DSPC (Fig. 6B), which correlated with the low amount of helical structure. However, the 208 nm band was severely reduced in the DDPC, DMPC and unsaturated POPC samples (Fig. 6A–C). Cholesterol did not prevent insertion of maculatin 1.1 in DMPC nor in POPC membranes. However, negatively charged

**Table 2**

Maculatin 1.1<sup>a</sup> secondary structure analyses<sup>b</sup> in SUV environment.

System (T <sub>m</sub> °C) [18,19]	T (°C) below T <sub>m</sub>	% $\alpha$ Helix	T (°C) above T <sub>m</sub>	% $\alpha$ Helix
Buffer	20	7	37	4
<i>Saturated neutral systems</i>				
SUV DHPC	–	–	37	4
SUV DDPC	–	–	37	52
SUV DLPC (–1)	–	–	37	65
SUV DMPC (23)	10	66	37	64
SUV DPPC (41)	20	28	60	61
SUV DSPC (55)	37	23	60	37
<i>Unsaturated neutral systems</i>				
SUV POPC (–2)	–	–	37	56
SUV DOPC (–20)	–	–	37	52
SUV egg PC (–5)	–	–	37	52
<i>Cholesterol containing systems<sup>c</sup></i>				
SUV DMPC/Chol	10	–	37	–
SUV DPPC/Chol	20	9	60	36
SUV POPC/Chol	–	–	37	58
<i>Saturated anionic systems</i>				
SUV DMPA (50)	37	63	60	58
SUV DMPS (35)	20	62	45	69
SUV DPPS (54)	37	59	60	64
SUV DMPG (23)	10	65	37	63
SUV TMCL (42)	20	62	60	65
<i>Unsaturated anionic systems</i>				
SUV POPS (14)	10	71	37	71
SUV POPG (–2)	–	–	37	66
SUV <i>E. coli</i> PG	–	–	37	64
SUV <i>E. coli</i> CL	–	–	37	62

<sup>a</sup> The peptide concentration was 30  $\mu$ M. Buffer composition: 30  $\mu$ M in Tris 10 mM/NaCl 20 mM buffer pH=7.3. The lipid to peptide molar ratio was 30:1 for all systems.

<sup>b</sup> Deconvoluted with ContinLL algorithm and SDP 48 basis-set (CDPro software).

<sup>c</sup> 30% molar ratio of cholesterol to lipid. Systems containing cholesterol were measured above and below the T<sub>m</sub> of the lipid in the absence of cholesterol, where applicable.

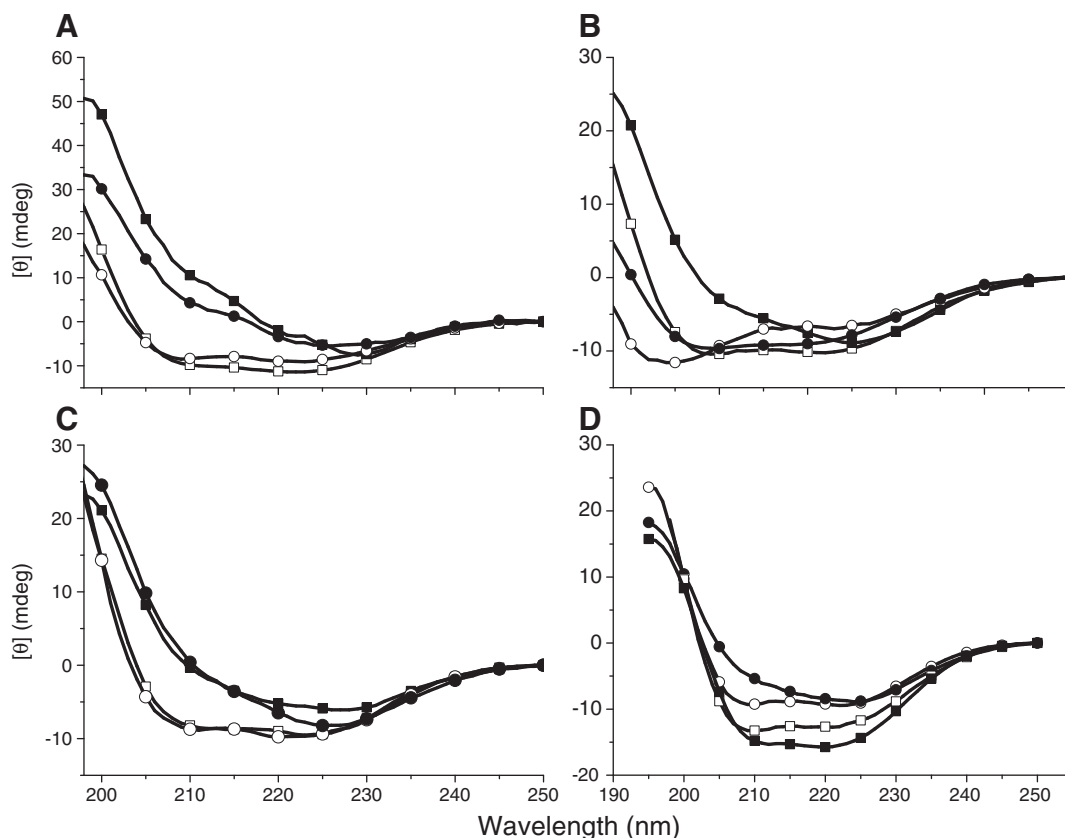


**Fig. 6.** OCD (filled symbols) and CD (open symbols) spectra of maculatin 1.1 in: (A) DMPC (squares), DMPC/Chol (circles); (B) DDPC (squares), DSPC (circles); (C) POPC (squares), POPC/Chol (circles); and (D) *E. coli* PG (squares), DMPG (circles). Experiments done at 37 °C. For OCD, 4 glass plate orientations and 3 accumulations were averaged.

phospholipids locked the peptide on the surface of the bilayers as observed in the CD spectra of DMPG and *E. coli* PG samples (Fig. 6D).

#### 4. Discussion

The behaviour of maculatin 1.1, a natural antimicrobial peptide disrupting specifically bacterial membranes, was used to demonstrate that the lipid composition used for *in vitro* studies must be chosen with care [25–27]. We report here only membranes composed of single phospholipids to serve as a basis for future studies of complex lipid mixtures.

##### 4.1. Maculatin 1.1 conformation and insertion in zwitterionic membranes

Phosphatidylcholines are the major lipids found in eukaryotic cell membranes. Therefore, model membranes composed of DMPC have been used to mimic eukaryotic membranes due to their inexpensive cost and well-characterised properties. However, *in vivo* data often differ from *in vitro* data using this simple model. For instance, maculatin 1.1 is weakly active against eukaryotic cells but is strongly bactericidal, especially against Gram-positive bacteria which possess high amounts of anionic lipids. In DMPC LUV, maculatin adopted its active amphipathic helix conformation and in planar DMPC bilayers, was observed to insert parallel to the membrane's normal. The addition of cholesterol, only present in eukaryotic cells, did not modify the peptide interaction with DMPC bilayers. However, in bilayers of longer saturated acyl chain phospholipids, maculatin was mainly unstructured with cholesterol further lowering the  $\alpha$ -helical content.

Maculatin 1.1 formed an amphipathic helix upon insertion into the hydrophobic core of neutral membranes of a favourable thickness. This is supported by the low amount of helix obtained in DPC micelles, which have the same headgroup but more highly curved surface and an

approximately 32 Å hydrophobic thickness. Since SUV produced a similar interaction to LUV but with a ~10% decrease in helical structure, curvature is not a major parameter regulating maculatin 1.1 secondary structure. The helical structure of maculatin 1.1 for PC systems of increasing acyl chain length is plotted against the corresponding hydrophobic thickness [28,29] in Fig. 7. Apparently, there is an optimal hydrophobic thickness range occurring between 20 Å and 26 Å. Comparing the optimal hydrophobic thickness to the length of an  $\alpha$ -helix composed of ~15 amino acids (73% of 21 residues), a good match can be observed between the peptide (22.5 Å) and the membrane thickness.

Biological membranes are composed of mixed acyl chains usually between 16 and 22 carbons, with a saturated/unsaturated lipid ratio close to 0.5 [30]. While maculatin 1.1 conformation with POPC, DOPC

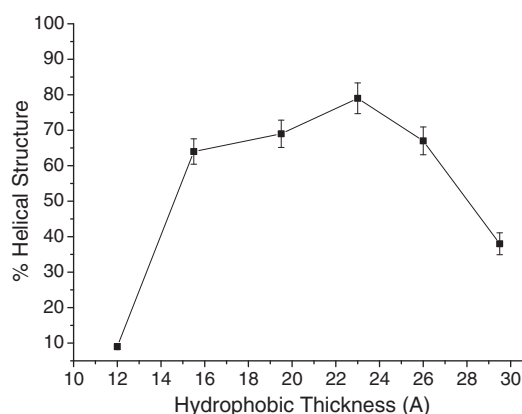


**Fig. 7.** Helical structure (%) of maculatin 1.1 in unsaturated PC systems of different chain lengths plotted against corresponding fluid-phase bilayer hydrophobic thicknesses. Helical structure generated by deconvolution of CD spectra using SMP56 basis-set and ContinLL algorithm on CDPPro software package.

and egg PC bilayers showed a gradual decrease in  $\alpha$ -helix, the peptide maintained a high degree of  $\alpha$ -helical structure near 60%. The hydrophobic thicknesses of these unsaturated membranes vary slightly around 26 Å and may explain the ability of maculatin 1.1 to insert into the hydrophobic core of unsaturated membranes as well. Taking into account the small effect of cholesterol on the peptide structure and location, it seems that ordered membrane cores were not a more favourable environment for the peptide. Hence, mimicking eukaryotic membranes with PC bilayers may not be relevant to assess the toxicity of antimicrobial peptides [6].

#### 4.2. Maculatin 1.1 surface interaction with anionic membranes

Prokaryotic membranes, and especially Gram-positive bacteria, possess a high amount of anionic lipids, conferring a negatively charged surface potential differentiating them from eukaryotic neutral membranes. All anionic phospholipids bilayers with saturated, unsaturated or mixed chains induced a strong structuring effect on maculatin 1.1: rigid or fluid chains, bilayer or micelle, small or bulky headgroups with hydrogen bonding capacity did not significantly change the amount of  $\alpha$ -helix. The peptide was found on the surface of DMPG and POPG bilayers, with no evidence of insertion into the hydrophobic core. The hydrophobic thickness did not play a critical role in the peptide interaction with anionic lipids, and the electrostatic forces would maintain maculatin 1.1 on the membrane surface. In general, the peptide was slightly more structured than with PC lipids and possibly the higher affinity of maculatin 1.1 for negatively charged bacterial membranes than eukaryotic cells may explain the antimicrobial activity.

## 5. Conclusions

In order to understand the key properties allowing antimicrobial peptides to discern between eukaryotic and prokaryotic cells, better models of cell membranes are needed. The antimicrobial peptide, maculatin 1.1, is effective against Gram-positive bacteria and exhibited a strong interaction with anionic bilayers. While hydrophobic mismatch was crucial in neutral bilayer systems, insertion into charged bilayers was not observed. Although single lipid systems are not sufficient to mimic biological membranes the peptide conformation was dependent on the homeoviscous nature of the membrane. Bilayers composed of binary and ternary lipid mixtures are under investigation to better mimic relevant cell membranes.

## Acknowledgements

This project was funded by the University of Melbourne MRGS and SEED grants. The authors would like to thank Dr. J. Gehman for helpful discussions.

## References

- [1] P.R. Cullis, D.B. Fenske, M.J. Hope, *Physical Properties and Functional Roles of Lipids in Membranes*, Elsevier Science B.V., 1996.
- [2] W. Dowhan, Molecular basis for membrane phospholipid diversity: why are there so many lipids? *Annu. Rev. Biochem.* 66 (1997) 199–232.
- [3] R.M. Epand, S. Rotem, A. Mor, B. Berno, R.F. Epand, Bacterial membranes as predictors of antimicrobial potency, *J. Am. Chem. Soc.* 130 (2008) 14346–14352.
- [4] D.I. Fernandez, J.D. Gehman, F. Separovic, Membrane interactions of antimicrobial peptides from Australian frogs, *Biochim. Biophys. Acta* 1788 (2009) 1630–1638.
- [5] N.K. Burgess, T.P. Dao, A.M. Stanley, K.G. Fleming, Beta-barrel proteins that reside in the *Escherichia coli* outer membrane in vivo demonstrate varied folding behavior in vitro, *J. Biol. Chem.* 283 (2008) 26748–26758.
- [6] J.T. Cheng, J.D. Hale, M. Elliott, R.E. Hancock, S.K. Straus, The importance of bacterial membrane composition in the structure and function of aurein 2.2 and selected variants, *Biochim. Biophys. Acta* 1808 (2011) 622–633.
- [7] R.M. Epand, R.F. Epand, Lipid domains in bacterial membranes and the action of antimicrobial agents, *Biochim. Biophys. Acta* 1788 (2009) 289–294.
- [8] J. Huang, G.W. Feigenson, A microscopic interaction model of maximum solubility of cholesterol in lipid bilayers, *Biophys. J.* 76 (1999) 2142–2157.
- [9] J. Huang, J.T. Buboltz, G.W. Feigenson, Maximum solubility of cholesterol in phosphatidylcholine and phosphatidylethanolamine bilayers, *Biochim. Biophys. Acta* 1417 (1999) 89–100.
- [10] M.A. Sani, C. Loudet, G. Grobner, E.J. Dufourc, Pro-apoptotic bax- $\alpha$ 1 synthesis and evidence for beta-sheet to alpha-helix conformational change as triggered by negatively charged lipid membranes, *J. Pept. Sci.* 13 (2007) 100–106.
- [11] N. Sreerama, R.W. Woody, Estimation of protein secondary structure from circular dichroism spectra: comparison of CONTIN, SELCON, and CDSSTR methods with an expanded reference set, *Anal. Biochem.* 287 (2000) 252–260.
- [12] N. Sreerama, S.Y. Venyaminov, R.W. Woody, Estimation of protein secondary structure from circular dichroism spectra: inclusion of denatured proteins with native proteins in the analysis, *Anal. Biochem.* 287 (2000) 243–251.
- [13] N. Sreerama, R.W. Woody, On the analysis of membrane protein circular dichroism spectra, *Protein Sci.* 13 (2004) 100–112.
- [14] M.S. Balla, J.H. Bowie, F. Separovic, Solid-state NMR study of antimicrobial peptides from Australian frogs in phospholipid membranes, *Eur. Biophys. J.* 33 (2004) 109–116.
- [15] M. Sinensky, Homeoviscous adaptation—a homeostatic process that regulates the viscosity of membrane lipids in *Escherichia coli*, *Proc. Natl. Acad. Sci. U.S.A.* 71 (1974) 522–525.
- [16] A. Zaritsky, A.H. Parola, M. Abdah, H. Masalha, Homeoviscous adaptation, growth rate, and morphogenesis in bacteria, *Biophys. J.* 48 (1985) 337–339.
- [17] D. Marsh, Liquid-ordered phases induced by cholesterol: a compendium of binary phase diagrams, *Biochim. Biophys. Acta* 1798 (2010) 688–699.
- [18] S.A. Sanchez, M.A. Tricerri, G. Ossato, E. Gratton, Lipid packing determines protein-membrane interactions: challenges for apolipoprotein A-I and high density lipoproteins, *Biochim. Biophys. Acta* 1798 (2010) 1399–1408.
- [19] D. Marsh, *CRC Handbook of Lipid Bilayer*, CRC Press, Boca Raton, Florida, 1990.
- [20] O.H. Griffith, P.C. Jost, *Lipid-protein Interactions*, Wiley Interscience, 1982.
- [21] T. Baumgart, B.R. Capraro, C. Zhu, S.L. Das, Thermodynamics and mechanics of membrane curvature generation and sensing by proteins and lipids, *Annu. Rev. Phys. Chem.* 62 (2011) 483–506.
- [22] J. Burck, S. Roth, P. Wadhwani, S. Afonin, N. Kanithasen, E. Strandberg, A.S. Ulrich, Conformation and membrane orientation of amphiphilic helical peptides by oriented circular dichroism, *Biophys. J.* 95 (2008) 3872–3881.
- [23] A.H. Clayton, W.H. Sawyer, Oriented circular dichroism of a class A amphipathic helix in aligned phospholipid multilayers, *Biochim. Biophys. Acta* 1467 (2000) 124–130.
- [24] Y. Wu, H.W. Huang, G.A. Olah, Method of oriented circular dichroism, *Biophys. J.* 57 (1990) 797–806.
- [25] J.T. Cheng, J.D. Hale, M. Elliot, R.E. Hancock, S.K. Straus, Effect of membrane composition on antimicrobial peptides aurein 2.2 and 2.3 from Australian southern bell frogs, *Biophys. J.* 96 (2009) 552–565.
- [26] Y. Ishitsuka, D.S. Pham, A.J. Waring, R.I. Lehrer, K.Y. Lee, Insertion selectivity of antimicrobial peptide protegrin-1 into lipid monolayers: effect of head group electrostatics and tail group packing, *Biochim. Biophys. Acta* 1758 (2006) 1450–1460.
- [27] F. Neville, M. Cahuzac, O. Konovalov, Y. Ishitsuka, K.Y. Lee, I. Kuzmenko, G.M. Kale, D. Gidalevitz, Lipid headgroup discrimination by antimicrobial peptide LL-37: insight into mechanism of action, *Biophys. J.* 90 (2006) 1275–1287.
- [28] B.A. Cornell, F. Separovic, Membrane thickness and acyl chain length, *Biochim. Biophys. Acta* 733 (1983) 189–193.
- [29] B.A. Lewis, D.M. Engelman, Lipid bilayer thickness varies linearly with acyl chain length in fluid phosphatidylcholine vesicles, *J. Mol. Biol.* 166 (1983) 211–217.
- [30] E.C. Borsonelo, J.C. Galduroz, The role of polyunsaturated fatty acids (PUFAs) in development, aging and substance abuse disorders: review and propositions, *Prostaglandins Leukot. Essent. Fatty Acids* 78 (2008) 237–245.